Effect of Microstructural and Physical Mechanisms on Mechanical Properties of Single-Phase Steels

Gérald Franz, Farid Abed-Meraim, Tarak Ben Zineb

Effect of microstructural and physical mechanisms on mechanical properties of single-phase steels

Gérald Franz[1], Farid Abed-Meraim[2,3], Tarak Ben Zineb[4]

[1]LTI, EA 3899 – IUT Amiens, Avenue des Facultés – Le Bailly, 80025 Amiens Cedex 1, France
[2]LEM3, UMR CNRS 7239 – Arts et Métiers ParisTech, 4 rue Augustin Fresnel, 57078 Metz Cedex 3, France
[3]DAMAS, Laboratory of Excellence on Design of Alloy Metals for low-mAss Structures, Université de Lorraine, France
[4]LEMTA, UMR CNRS 7563 – Université de Lorraine, 2 rue Jean Lamour, 54500 Vandœuvre-lès-Nancy, France

The current work aims to investigate the impact of microstructural and physical mechanisms on the macroscopic behavior and ductility of single-phase steels. For this purpose, an advanced multiscale model, accounting for intragranular microstructure development and evolution, is coupled with a formability limit criterion based on bifurcation theory. The overall response for polycrystalline aggregates is obtained from a large-strain elastic–plastic single crystal constitutive law, using a self-consistent scale-transition scheme. This approach takes into account essential microstructural aspects such as initial and induced textures, dislocation densities, softening mechanisms so that the behavior during complex loading paths is properly described. Focus will be placed here on the relationship between intragranular microstructure of B.C.C. steels and their ductility. The model allows interesting qualitative study in terms of formability limits for various dislocation networks, during monotonic loading tests applied to single-phase steels, with the aim of helping in the design of new materials.

Keywords: Micromechanics, Intragranular Substructure, Ductility.

1. INTRODUCTION

It is now well-known that plastic deformation of thin metal sheets induces strain-path changes, which often result in softening/hardening macroscopic effects that may considerably influence the strain distribution and may lead to flow localization and material failure. These phenomena are believed to originate during the evolution of intragranular microstructure.

In this regard, the development of accurate and reliable constitutive models that are well-suited to sheet metal forming simulations requires a careful description of the most important sources of anisotropy, e.g., plastic slip processes, intragranular substructure changes and texture development.

The main objective of the present work is to investigate the effect of microstructural mechanisms on mechanical properties and formability of single-phase steels. To this end, a material instability criterion has been coupled with a crystal plasticity-based constitutive model that includes an accurate description of the heterogeneous dislocation distribution and that has been incorporated into a self-consistent scale-transition scheme. Only the microscopic modeling and plastic instability criterion are outlined here, the complete multiscale model has been presented in Franz et al.[1]. Its ability to describe the evolution of the intragranular heterogeneous dislocation distribution and to accurately reproduce the macroscopic behavior of single-phase polycrystalline steels during monotonic and sequential loading paths has been shown.

A qualitative strain localization analysis for a 1000-grain polycrystal that represents an IF–Ti ferritic single-phase steel is carried out, which allows us to emphasize the relationship between microstructure and ductility.

*Email Address: farid.abed-meraim@ensam.eu

2. INTRAGRANULAR MICROSTRUCTURE MODELING

The microscopic model adopted here, based on experimental observations on B.C.C. grains, is inspired by the works of Peeters et al.[2,3]. In this modeling, hardening is described through several families of dislocation densities and their evolution equations.

During plastic deformation, an intragranular microstructure develops, consisting of straight planar dislocation walls, and of statistically stored dislocations in the cells. The spatially heterogeneous distribution of dislocations inside the grain is represented by three types of local dislocation densities (see Fig. 1).

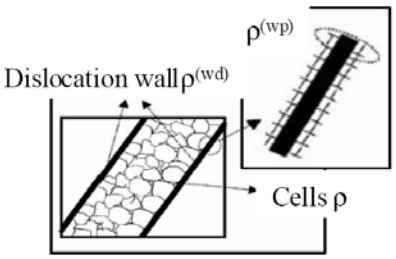

Fig.1. Schematic representation of the heterogeneous dislocation microstructure

The dislocations stored randomly inside cells are represented by a single local dislocation density ρ. Two other types of dislocation densities are associated with the dense dislocation walls: the density of immobile dislocations stored in the dislocation sheets ρ^{wd}, and the local, directionally movable or polarized dislocation density ρ^{wp}. The latter is assumed to have a sign that reproduces asymmetry in slip resistance.

The model will construct at most two families of dislocation sheets parallel to the {110} planes on which the highest and second highest slip activity rate occur, in agreement with experimental observations on B.C.C. crystals (see Fig. 2).

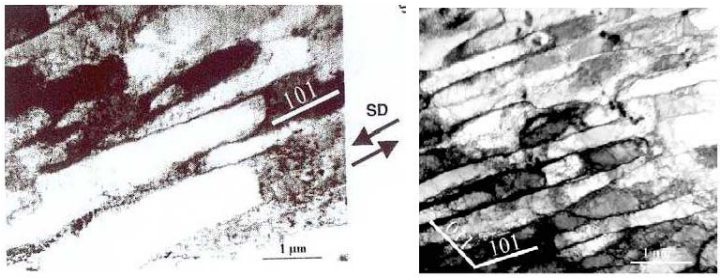

Fig.2. Longitudinal plane view TEM micrographs (after Peeters et al.[3]): (left) of a (-27.7, 133.5, 51.7°)-oriented grain in a 15% sheared specimen with SD parallel to RD and SPN parallel to TD, and (right) of a (-41.6, 135.2, 38.7°)-oriented grain in a 30% sheared specimen with SD parallel to RD and SPN parallel to TD

During plastic deformation, the mobile dislocations may get either trapped inside cells and in walls, or get annihilated with immobile dislocations of opposite sign or through pencil glide. These phenomena are accounted for through the evolution equations of the three types of dislocation densities, using two different terms of hardening, which express the mechanisms of immobilization.

In order to account for the effect of the pre-existing microstructure and thus for the strain-path history of the material, the model will necessarily have to distinguish the evolution of currently existing dislocation walls from that of previously existing dislocation sheets.

The evolution equation associated with the intensity of local immobile dislocation density for each of the existing generated dislocation sheets can thus be expressed as

$$\dot{\rho}_i^{wd} = \frac{1}{b}\left(I^{wd}\sqrt{\rho_i^{wd}} - R^{wd}\rho_i^{wd} \right)\dot{\Gamma}_i \qquad (1)$$

with b representing the magnitude of the Burgers vector, $\dot{\Gamma}_i$ the total slip rate on the crystallographic plane on which the i^{th} greatest slip activity occurs, I^{wd} and R^{wd} the immobilization and the recovery parameter, respectively.

The evolution of the polarized dislocation density associated with each current wall can be expressed in the same manner as the previous evolution law (1):

$$\dot{\rho}_i^{wp} = \left(\operatorname{sign}\left(\phi_i^{wp}\right) I^{wp}\sqrt{\rho_i^{wd} + \left|\rho_i^{wp}\right|} - R^{wp}\rho_i^{wp} \right)\left|\phi_i^{wp}\right| \qquad (2)$$

In the equation above, $\phi_i^{wp} = \sum_{s=1}^{n} \frac{\dot{\gamma}^s}{b}\mathbf{m}^s \cdot \mathbf{n}_i^w$ is the net flux of the dislocations covering the boundaries of each current dislocation sheet i from all the slip systems non-coplanar to that family i. n denotes the number of slip systems (n = 24 for B.C.C. crystals). The slip rate $\dot{\gamma}^s$ on slip system s can be positive or negative in order to account for the different slip directions on a particular slip system. $\mathbf{m}^s$ represents the unit vector assigned to the slip direction of system s, and $\mathbf{n}_i^w$ corresponds to the unit vector perpendicular to the existing generated dense sheet i. I^{wp} and R^{wp} are respectively the immobilization and the recovery parameter.

During a reverse test, the polarity dislocations that have already been stuck along dense sheets can easily move away and be annihilated by dislocations of opposite sign. Accordingly, the net dislocation flux ϕ_i^{wp} associated with a family of current dense walls i is reversed. The evolution of the polarized dislocation density associated with each of the existing generated dislocation sheets will thus be expressed by the following equation:

$$\dot{\rho}_i^{wp} = -R_{rev}\rho_i^{wp}\left|\phi_i^{wp}\right| \qquad (3)$$

where R_{rev} denotes the recovery parameter of mobile dislocations associated with the dense dislocation sheet family i.

New slip systems may be activated consecutively to strain-path changes or when a grain rotates towards a stable orientation. New families of dense walls

corresponding to the current strain path will be thus formed and, at the same time, the previously generated dislocation sheets will be also disintegrated according to:

$$\dot{\rho}_i^{wd} = -\frac{R_{ncg}}{b}\rho_i^{wd}\dot{\Gamma}_{new}, \qquad \dot{\rho}_i^{wp} = -\frac{R_{ncg}}{b}\rho_i^{wp}\dot{\Gamma}_{new} \tag{4}$$

where $\dot{\Gamma}_{new}$ is the total slip rate on both of the crystallographic planes containing the highest slip activity, and R_{ncg} is an annihilation parameter characterizing the destruction of former dense dislocation sheets.

Considering that the isotropic hardening in the material is attributable to the dislocations statistically stored in the cell interiors, the evolution of the dislocation density is thus expressed by the summation of a storage term and an annihilation term, according to the Kocks law.

Furthermore, it was experimentally observed that the dislocation density statistically stored in the cell interiors tends to decrease during load reversal. This can be explained by the activation in the opposite sense of most of the same slip systems that were active during prestrain. We assume that the directionally movable dislocations, responsible for the polarity of the dense walls, are likely to be at the origin of this annihilation. This is why an additional source of annihilation is added to account for this phenomenon as follows

$$\dot{\rho} = \frac{1}{b}\left\langle \left(I\sqrt{\rho} - R\rho\right)\sum_{s=1}^{n}\left|\dot{\gamma}^s\right| - \Psi R_2 \frac{\rho^{bausch}}{2\rho_{sat}^{wp}}\sum_{s=1}^{n}\left|\dot{\gamma}^s\right| \right\rangle \tag{5}$$

where I and R are, respectively, the immobilization parameter and the recovery parameter associated with the randomly distributed dislocation network. $\langle y\rangle = y$ if $y > 0$; $\langle y\rangle = 0$ otherwise. To activate the additional term of annihilation, the switch parameter Ψ will take binary values ($\Psi = 0$ or $\Psi = 1$), depending on whether or not there is reversal of the flux associated with a family of currently generated walls. The importance of the annihilation of the dislocations statistically stored in the cell interiors by the remobilized directionally movable dislocations associated with the dense dislocation sheets will be reflected by parameter R_2. The value of ρ^{bausch} will be different according to the number of reversed fluxes.

The critical resolved shear stress on each slip system s includes the contributions of isotropic hardening, latent hardening and polarity, which are related to the three above-defined dislocation densities. The resulting critical resolved shear stress is then given by

$$\tau_c^s = \tau_{c0}^s + (1-f)\alpha\mu b\sqrt{\rho} + f\sum_{i=1}^{6}\alpha\mu b\left(\sqrt{\rho_i^{wd}}\left|\mathbf{m}^s\cdot\mathbf{n}_i^w\right| + \left\langle\sqrt{\left|\rho_i^{wp}\right|}\left(\mathbf{m}^s\cdot\mathbf{n}_i^w\right)\mathrm{sign}\left(\rho_i^{wp}\right)\right\rangle\right) \tag{6}$$

where f is the volume fraction of the dislocation sheets, α the dislocation interaction parameter, μ the shear modulus and τ_{c0} the initial critical resolved shear stress.

3. SIMULATION RESULTS – MACROSCOPIC BEHAVIOR OF POLYCRYSTALLINE SINGLE-PHASE STEEL

In order to derive the overall macroscopic polycrystalline behavior starting from knowledge of the behavior of individual grains, the self-consistent scale-transition scheme in the sense of Hill[4] is adopted.

In this section, the results obtained with the proposed model are compared to experimental tests (see Fig. 3). Several sequential mechanical tests have been performed for an IF–Ti ferritic single-phase steel. The identified parameters for this steel are reported in Table 1 below. The identification procedure is explained in Franz et al.[1]

Table.1. Identified parameters for the IF–Ti steel.

I	R(m)	I^{wd}	R^{wd}(m)
2.4×10^{-2}	2.2×10^{-9}	2×10^{-1}	1.3×10^{-10}
I^{wp}	R^{wp}(m)	R_{ncg}(m)	R_{rev}(m)
2.4×10^{-2}	1.8×10^{-9}	1×10^{-9}	1×10^{-10}
R_2(m)	f	τ_{c0}[110](MPa)	τ_{c0}[112](MPa)
1×10^{-10}	0.2	55	55

As observed in Fig. 3, the simulation results obtained with the multiscale model are in agreement with those of experimental tests. Therefore, the proposed multiscale model is able to reproduce the elastic–plastic behavior of single-phase polycrystalline materials.

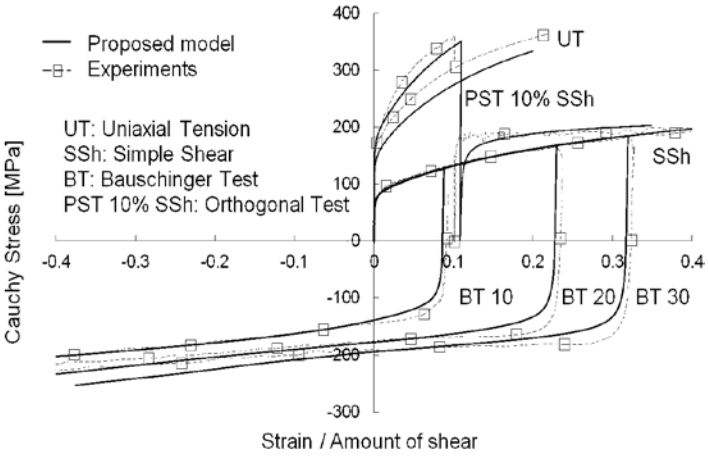

Fig.3. Comparison model/experiments for the stress–strain response of an IF–Ti steel during various strain paths performed perpendicular to RD

4. MODELING OF FORMABILITY LIMITS

The Rudnicki–Rice criterion[5,6] corresponds to a bifurcation associated with admissible jumps of strain and stress rates across a localized shear band (as schematized in Fig. 4).

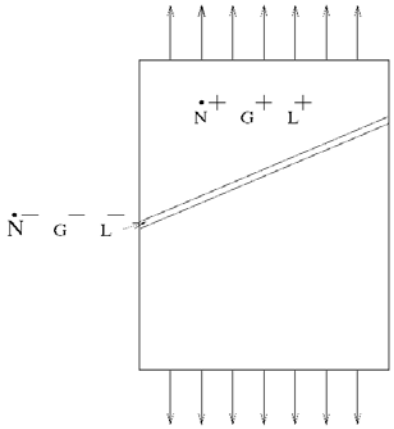

Fig.4. Schematic representation of strain localization along a shear band

Because field equations have to be satisfied, and because the velocity gradient is discontinuous across the localization band, a kinematic condition for the strain rate jump must be verified. Also, the continuity of the stress rate vector has to be verified for the forces along the localization band. For more details, the interested reader may refer to Franz et al.[7].

Combining all of these conditions, a localization criterion, which will be used as a ductility limit indicator, can be easily expressed as a function of the only macroscopic elastic–plastic tangent modulus by:

$$\det\left(\boldsymbol{\upsilon}\cdot\mathbf{L}\cdot\boldsymbol{\upsilon}\right)=0 \tag{7}$$

In the above condition, corresponding to the singularity of the acoustic tensor and interpreted as loss of ellipticity of the associated boundary value problem, $\boldsymbol{\upsilon}$ is the unit vector normal to the localization band (see Fig. 4), and $\mathbf{L}$ is the effective elastic–plastic tangent modulus for the polycrystalline aggregate.

5. SIMULATION RESULTS – IMPACT OF MICROSTRUCTURAL AND PHYSICAL MECHANISMS ON DUCTILITY

It is interesting to qualitatively investigate the impact of microstructural mechanisms on ductility, which can be advantageously used in the design of new materials in order to optimize their formability and mechanical properties in-use. In this process, the effect on ductility of the material parameters, which are associated with elementary physical mechanisms at the microscale, will be analyzed during monotonic loading tests. More specifically, the impact of some selected physical parameters on the three extreme points of the Forming Limit Diagram (i.e., uniaxial tension, plane strain tension, and balanced biaxial extension) is shown through Fig. 5 to Fig. 8. The selected parameters correspond respectively to the two specific parameters of the model, *I* and *R*, which are associated with the randomly distributed dislocation network, the initial critical resolved shear stress τ_{c0}, and the volume fraction *f* of dislocation sheets.

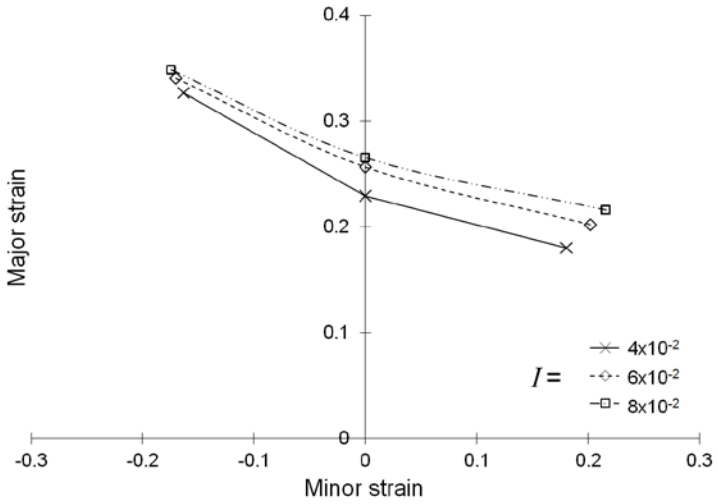

Fig.5. Impact of the immobilization parameter *I* on ductility limits of a single-phase steel

Assuming that the internal substructure is disorganized signifies that dislocations are distributed in a totally random way. In order to reproduce this assumption, all the values of the model parameters are set at zero, except for the initial critical resolved shear stress τ_{c0}, the immobilization parameter *I* and the recovery parameter *R*.

In these conditions, the microscopic modeling comes down to Eq. (5) for the evolution of the randomly distributed dislocations. This equation reveals that it contains two terms of opposite sign corresponding, respectively, to storage and annihilation of dislocations. The immobilization parameter *I* defines the number of dislocations that are going to be trapped inside cells. Larger values of this parameter induce more obstacles to slip and consequently an increase in hardening leading to better ductility. This trend is clearly reflected by the proposed model, as shown in Fig. 5.

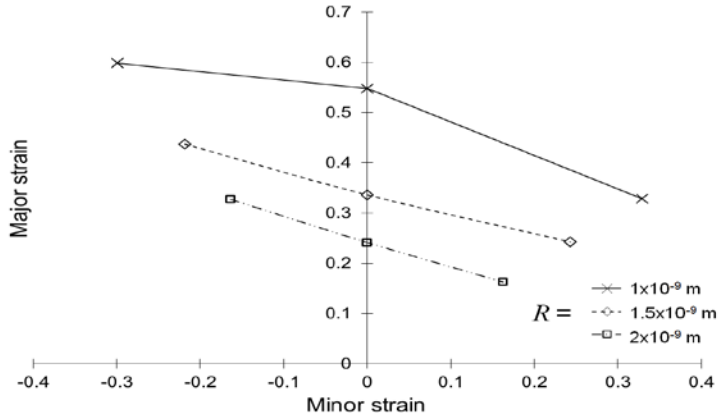

Fig.6. Impact of the recovery parameter *R* on ductility limits of a single-phase steel

In the same way, the importance of annihilation of randomly distributed dislocations can be quantified by means of the recovery parameter *R*. Larger values of this parameter mean that more dislocations are going to disappear, making easier slip motion, which leads to overall softening of the material thus promoting early strain localization, as shown in Fig. 6.

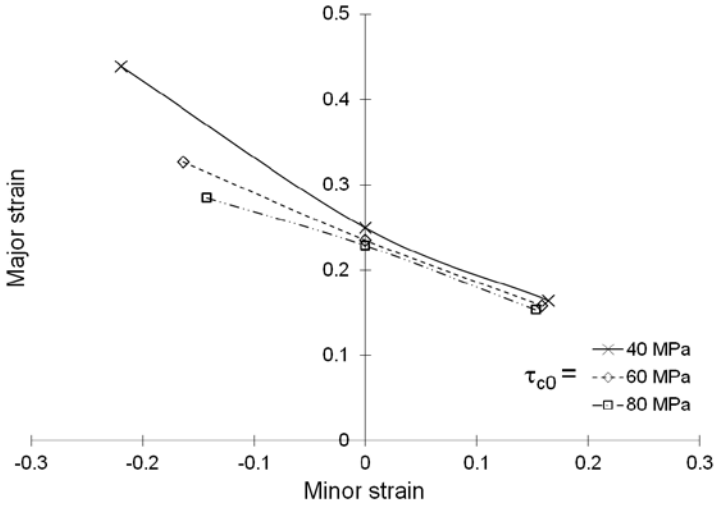

Fig.7. Impact of initial critical resolved shear stress τ_{c0} on ductility limits of a single-phase steel

As depicted in Fig. 7, a decrease in the initial critical resolved shear stress τ_{c0} leads to improvement of overall ductility. This result may be compared to the Luft work[8], reporting that a decrease in the temperature during uniaxial tension on single crystals of molybdenum induces an increase in the elastic limit and thus a drop in ductility. The initial critical resolved shear stress τ_{c0} being directly linked to the elastic limit during uniaxial tensile test, the effects found by the proposed model are in agreement with Luft's results[8].

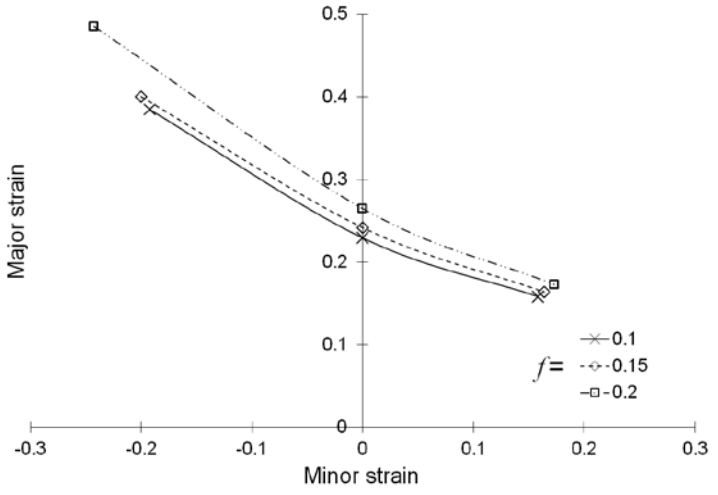

Fig.8. Impact of volume fraction *f* of walls on ductility limits of a single-phase steel

Finally, as suggested by Fig. 8, an increase in the volume fraction *f* of the dislocation walls improves ductility. This is explained by the fact that increasing the presence of dislocation sheets, which are parallel to the crystallographic planes on which the slip activity is greatest, means that fewer dislocations are likely to act as obstacles to the slip of other dislocations.

6. CONCLUSIONS

The plastic instability criterion based on bifurcation theory first proposed by Rice has been applied to elastic–plastic tangent moduli derived from a large-strain micromechanical model combined with a self-consistent scale-transition scheme. This multiscale model incorporates microscopic modeling that allows the formation and evolution of intragranular dislocation patterns on strain paths to be precisely reproduced.

The resulting theoretical and numerical tool proves to be useful, as it allows the ductility of new grades of steels to be predicted at the very early stages of their design. Additional features of the tool are that it allows the formability of different materials to be compared, which may serve for hierarchical classification of metals with regard to ductility. This prediction tool also allows the impact of microstructural parameters on ductility to be emphasized. Therefore, it could be used to optimize the ductility of new steels or to design materials with desired formability and in-use properties.

REFERENCES

[1] G. Franz, F. Abed-Meraim, T. Ben Zineb, X. Lemoine, M. Berveiller. Role of intragranular microstructure development in the macroscopic behavior of multiphase steels in the context of changing strain paths, Materials Science and Engineering A, 517 (2009) 300-311.

[2] B. Peeters, M. Seefeldt, C. Teodosiu, S.R. Kalidindi, P. Van Houtte, E. Aernoudt. Work-hardening/softening behaviour of b.c.c. polycrystals during changing strain paths: I. An integrated model based on substructure and texture evolution, and its prediction of the stress–strain behaviour of an IF steel during two-stage strain paths, Acta Materialia, 49 (2001) 1607-1619.

[3] B. Peeters, B. Bacroix, C. Teodosiu, P. Van Houtte, E. Aernoudt. Work-hardening/softening behaviour of b.c.c. polycrystals during changing strain paths: II. TEM observations of dislocation sheets in an IF steel during two-stage strain paths and their representation in terms of dislocation densities, Acta Materialia, 49 (2001) 1621-1632.

[4] R. Hill. Continuum micro-mechanics of elastoplastic polycrystals, Journal of the Mechanics and Physics of Solids, 13 (1965) 89-101

[5] J.W. Rudnicki, J.R. Rice. Condition for the localization of deformation in pressure-sensitive dilatant materials, Journal of the Mechanics and Physics of Solids, 23 (1975) 371-394.

[6] J.R. Rice. The localization of plastic deformation, in: W.T. Koiter (ed.), Proceeding of the 14th International Congress of Theoretical and Applied Mechanics, Amsterdam, (1976) 207-220.

[7] G. Franz, F. Abed-Meraim, T. Ben Zineb, X. Lemoine, M. Berveiller. Strain localization analysis using a multiscale model, Computational Materials Science, 45 (2009) 768-773.

[8] A. Luft. Microstructural processes of plastic instabilities in strengthened metals, Progress in Material Science, 35 (1991) 97-204.